A98-31664 ICAS-98-5,11,3

DESIGN AND ANALYSIS OF PROPELLERS FOR GENERAL AVIATION AIRCRAFT NOISE REDUCTION

Lorenz E. Drack* Lincoln A. Wood†

Abstract

A propeller design program has been developed for use by general aviation aircraft designers. Named SPONOP (Subsonic Propeller design for Noise and Performance), the primary motivation behind its development is to allow these designers to meet stringent noise regulations whilst maintaining or improving aircraft performance over off-the-shelf designs. The core of the design program is a two stage optimiser using simulated annealing and a gradient method to produce propellers which are optimal over the entire flight envelope, with constraints including maximum flyover noise level as specified by regulations and structural integrity in all operating conditions. The test case presented shows the optimiser's success in designing a propeller which allows a production aircraft to meet its noise certification requirement whilst improving the rate of climb during takeoff, range, maximum velocity and takeoff distance when compared to the same aircraft fitted with an off-the-shelf propeller.

Nomenclature

a_1	axial induced velocity
a_2	rotational velocity
C(r)	chord distribution across blade
C_t	thrust coefficient
C_q	torque coefficient
D	number of optimisation variables
dS	blade surface
dT	differential torque
E	state energy
F	Prandtl momentum loss factor
f(x)	cost function
g(x)	constraint function
h	acceptance probability
H	Hessian matrix
k	annealing time steps
L	Lagrangian multipliers
l_r	loading vector in radiation direction
M_n	Mach vector normal to blade
M_r	Mach vector in direction of radiation
N	number of blades
p(x,t)	acoustic pressure at observer x and time t
r	radiation vector
RPM	propeller revolutions per minute
THP	thrust horsepower
t^*	retarded time
T	temperature
V	freestream velocity
w	cost function weights
x	observer position
x	optimisation variables
x^*	optimal solution
y	source position in ground frame
λ	advance ratio

Introduction

It should first be noted that SPONOP is the design portion of a larger propeller analysis and design system simply known as PAD (see Figure 1). There are two other modules in PAD. One is an analysis program named SPINOP, which has been outlined in another paper by the authors [1]. The other is an acoustic testing procedures and spectral analysis module for the purpose of noise test data analysis.

The performance and noise analysis methods used by SPONOP differs from SPINOP in that they retain only the components required for design, and have also been optimised for speed, a primary concern in optimization problems of high dimensionality.

SPONOP was developed as part of a research program investigating the reduction of general aviation aircraft noise levels through the re-design of the propeller, whilst ensuring that aircraft performance is not compromised. This would enable designers to meet stringent noise regulations, as well as improving performance over off-the-shelf designs. The requirements of the software include ease of use, accuracy, easy modification to improve its accuracy or extend its capabilities, and finally it must arrive at a solution in an acceptable time on a desktop computer. In aid of this, SPONOP was written in MATLAB[2], making it portable across several platforms, namely PC, Macintosh and UNIX with only small modifications. The most computationally expensive portions were compiled in C++ and linked to MATLAB.

*PhD candidate, The Sir Lawrence Wackett Centre for Aerospace Design Technology, Royal Melbourne Institute of Technology, G.P.O Box 2476V, Melbourne, Vic 3001, AUSTRALIA. Email: wackett_centre@rmit.edu.au

†Research Leader, Maritime Systems and Survivability, Defence Science and Technology Organisation, Department of Defence, Australia. Adjunct Professor of Aerospace Engineering, RMIT.

21st ICAS Congress
13-18 September 1998
Melbourne, Australia

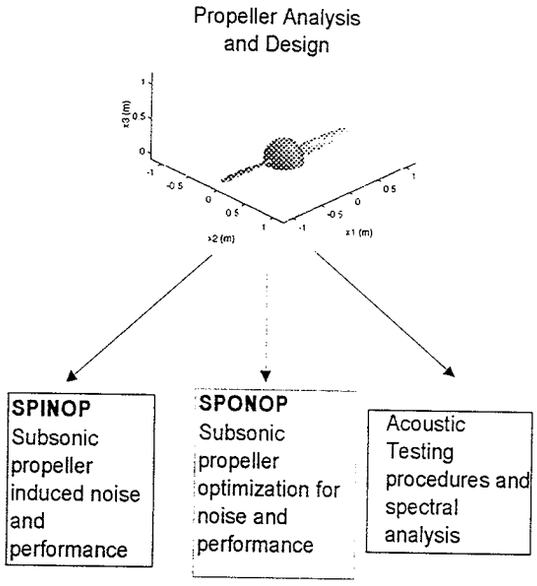

Figure 1 PAD

This paper will begin by presenting the optimization techniques used in SPONOP, followed by the construction of the objective function, including analysis techniques used, some of the techniques implemented to increase cost function evaluation speed and constraint handling. Finally, the optimiser's function will be verified and results will be discussed.

The Propeller Design Problem

The development of a quiet and efficient propeller poses several difficulties for the designer. The first is that these requirements are in conflict, meaning that a reduction in noise level is almost always accompanied by a reduction of propeller efficiency, and vica versa. In addition the propeller must perform well over a range of operating conditions, from static operation through to maximum speed flight. The design space thus has many local minima, and is also of a high dimensionality. This is combined with an objective function which requires a considerable amount of time to evaluate, due to numerous noise, performance and structural calculations for several design conditions. The result is a formidable design problem, which requires an optimiser capable of handling local minima and numerous design variables efficiently, without a good initial starting point to the problem.

Optimisation in SPONOP

The core of SPONOP is a two stage optimiser. The first stage uses simulated annealing[3] to find the region of the optimum. In many engineering design applications it is more important to find an acceptable solution in a reasonable amount of time rather than the global optimum, which is particularly applicable to problems of high dimensionality. Thus simulated annealing is used as it easily finds near optimal solutions quickly[4], allows the application of arbitrary boundary conditions and constraints, and is not thwarted by design spaces with nonlinearities and discontinuities.

Simulated annealing amounts to a stochastic search over a cost landscape, being directed by noise which is gradually reduced during convergence. The analogy to annealing derives from this noise being akin to the temperature of a cooling metal. Faster convergence (up to several orders of magnitude) is achieved by employing sophisticated cooling schedules, notably very fast simulated re-annealing[5]. Simulated annealing consists of three functional relationships. The first is the probability density of the design space g(x). Next is the probability density of accepting the next design proposal given the just previous one $h(\Delta E)$ (Equation 1).

$$h(\Delta E) = \exp\left(\frac{-\Delta E}{T}\right) \tag{1}$$

Lastly, there is the annealing schedule Tk. Fast annealing replaces a Boltzmann distribution with a Cauchy distribution (Equation 2) for the probability density of the design space permitting easier access to test local minima[6].

$$g_{ik} = \frac{T_{i0}}{\Delta x^{i^2} + T^2} \tag{2}$$

Very fast annealing accounts for differences in parameter dimensions, thus incorporating their varying sensitivities during annealing. It uses the following temperature schedule,

$$T_i(k) = T_{0i}\exp\left(-c_i k^{\frac{1}{D}}\right) \tag{3}$$

Reannealing involves rescaling the annealing time, thereby extending the search range of insensitive design variables, thus making available new sampling spaces. Adaptive simulated annealing (ASA), referring to very fast annealing and reannealing, has been found to be relatively efficient in terms of computational effort[7], for example, faring well against heuristic solutions to the travelling salesman problem. Additionally ASA affords convenience to the designer due to its reliability and ease of use. Its efficiency is most pronounced on problems of moderate to large dimensions.

The second stage of optimisation in SPONOP uses a gradient based optimiser to achieve rapid convergence in the region obtained from simulated annealing. The problem is now much more constrained than in the first stage as a near optimal solution has already been found. Thus employing a gradient based method is the most effective way to obtain a refined design, as these methods have a great dependency on their starting point.

The Kuhn-Tucker[8] equations (one of which is shown in Equation 4) defined the necessary conditions for optimality in a constrained optimization problem, which is the result of the cancelling of the gradients of the objective function and the active constraints at the solution point.

$$\nabla f(x^*) + \sum_{i=1}^{m} L_i^* \nabla g_i(x^*) = 0 \qquad (4)$$

The aim in constrained optimisation is to solve for the Lagrangian multipliers directly, and sequential quadratic programming (SQP)[9] is used here for this purpose. An approximation to the Hessian of the Lagrangian function is made at each major iteration using a quasi-Newton updating method. This in turn is used to generate a quadratic programming sub-problem the solution of which is used to generate a new search direction. The approximation to the Hessian provides the key to the optimiser's robustness, and the method of Broyden[10], Fletcher[11], Goldfarb[12] and Shanno[13] (BFGS) is used as a result of its applicability to a wide range of problems. The approximation to the Hessian is as follows,

$$H_{k+1} = H_k + \frac{q_k q_k^T}{q_k^T s_k} - \frac{H_k^T s_k^T}{s_k^T q_k^T s_k} \qquad (5)$$

$$s_k = x_{k+1} - x_k \qquad (6)$$

$$q_k = \nabla f(x_{k+1}) - \nabla f(x_k) \qquad (7)$$

In summary, we see that simulated annealing does the majority of the work in finding a good solution, with the gradient based method then being used to refine the design only when close to the optimum.

Program Structure

The following sub sections describe the inputs required from the designer, the construction of the cost function and constraint handling. A brief outline of the analytical methods used for calculation of noise and performance is also given.

Designer Inputs

The inputs required before optimisation is to begin are shown below,

- Geometry
  - propeller type: fixed pitch or constant speed
  - blade section type: ClarkY, RAF6, Eppler, AraD etc.
  - number of blades: support for two to eight blades
  - propeller tip shape: elliptical, round or square tip.
- Engine type: Complete power and fuel consumption tables are currently available for three Lycoming engines (250, 300 and 350 Hp variants).
- Aircraft variables:
  - velocity distribution at the propeller due to nacelle inflow blockage.
  - aircraft weight, efficiency, wing aspect ratio and wing area
- Range and endurance considerations:
  - fuel capacity
  - fuel reserve
  - cruise altitude
- Structural parameters:
  - blade material properties (material density, modulus of elasticity, fatigue strength)
  - hub counterweight geometry
- Calculation options:
  - noise calculation method
  - performance calculation method
  - specify cruise values or optimise

Optimization Variables

The optimization variables are a combination of geometrical and operational variables. For fixed pitch propellers, twist, thickness and chord distributions, radius and cruise velocity are used. For constant speed propellers, cruise RPM is used in addition to the above. Another option available to the designer is to specify the desired RPM and manifold pressure at cruise thus ensuring cruise operation at values which minimise engine fatigue.

The propeller geometry is represented by approximation functions in the case of the first optimiser stage. These functions allow satisfactory representation of a

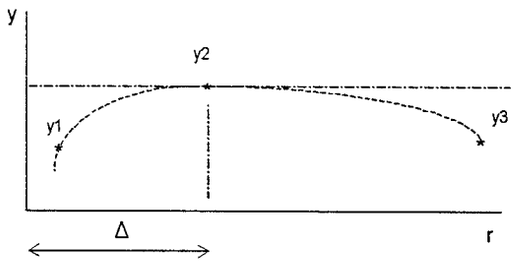

Figure 2 Chord representation in SPONOP

using only three or four variables. Twist and thickness are given by,

$$-A\log(r) + Br + C \tag{8}$$

which is a superposition of line and log curves. Chord is represented by root chord position, tip chord position, maximum chord position and finally displacement of maximum chord position from root (see Figure 2). Two piecewise polynomials are fitted to these points with equal gradients at the maximum chord position. When switching to the gradient based optimiser, the geometry is converted into discrete points along the blade for six slices. This geometry is then optimised with a maximum five percent fluctuation in their values, thus ensuring that the basic shape is maintained and subsequent optimiser convergence.

Cost Function

The design program must combine the following requirements in its cost function and meet them to varying degrees:

- short takeoff run
- large rate of climb at minimum power required for flight speed
- minimum rate of fuel flow
- highest maximum speed
- allowable noise level for fly-over noise test
- structural soundness in all operating conditions
- if required, specified cruise RPM and manifold pressure must be used

The designer chooses the order of importance of the primary cost function components maximum velocity, fuel flow, rate of climb at velocity for minimum power and takeoff distance. These are then sorted appropriately and combined using the following expression,

$$C = \frac{\exp(w)}{\sum \exp(w)} \cdot x \tag{9}$$

where w represents a vector of weights and x represents the primary cost function components. This function is chosen because the cost function component multiplier sums to one for an arbitrary weight range w, thus representing a percentage of importance for each component (the cost function components are normalized prior to inclusion in this function).

Objective Calculation

Analytical Methods Used

For accurate aerodynamic and noise prediction it is essential that the surface of the blade mesh be as smooth as possible. To achieve this, the program takes the section coordinates at each spanwise portion of the blade, and converts them to elliptic coordinates using an inverse Joukowski[14] transformation. The transformation "unwraps" the blade and allows accurate interpolation between points, particularly about the leading edge, which figures prominently in production of noise by the blade. This geometry is then used in subsequent performance and noise calculations.

To calculate blade loading one must first have accurate two dimensional lift and drag coefficients across the blade. The panel method[15] is used to calculate the inviscid potential flow around the airfoil. It yields the local velocity across the airfoil at a particular angle of attack. The pressure distribution is then found from which lift coefficient is derived. Boundary layer thicknesses are calculated from the integral displacement, momentum and energy equations[15] to produce the skin friction distribution across the airfoil for both the case of both a laminar boundary layer and a turbulent one. The drag coefficients are then obtained from the skin friction distribution.

Once aerodynamic properties have been established, propeller performance is calculated from the induced velocity field. Thrust and torque distributions are calculated using the method of Lock[16], which is an application of Goldstein's[17] theory. This is achieved by equating the increase in axial momentum to the thrust force,

$$dT = \frac{1}{2}V^2 NC(r)C_t = 4\pi\lambda^2 a_1(1+a_1)Fdr \tag{10}$$

and the increase of angular momentum to the torque force,

$$dQ = \frac{1}{2}V^2 NC(r)C_q = 4\pi\lambda r^3 \lambda a_2(1+a_1)Fdr \tag{11}$$

in an iterative solution based on axial and tangential components of the induced velocity.

The discrete tone noise of the propeller is calculated by the method of Farassat, using the subsonic formulation of his equations

$$4\pi p(\hat{x}, t) = \frac{\partial}{\partial t}\int_{\text{blade}}\left(\frac{M_n + l_r}{r|1-M_r|}\right)_\tau dS + \ldots$$

$$\frac{\partial}{\partial t}\int_{\text{blade}}\left(\frac{l_r}{r^2|1-M_r|}\right)_\tau dS \qquad (12)$$

This equation is derived from the Ffowcs Williams-Hawkings[18] equation, which itself is derived from Lighthill's[19] theory of aerodynamic sound. Farassat's method calculates the noise due to blade loading and thickness in the time domain and produces the pressure time history of the sound produced by the source(s) at the observer. The equation is solved at the emission time, otherwise known as the retarded time which requires the solution of the following

$$\tau^* - t + |\hat{x} - \hat{y}(\vec{\eta}, \tau^*)| = 0 \qquad (13)$$

A brief outline of the solution procedure of Farassat's' equation follows:

- Split revolution of one blade into several angular positions.
- Calculate retarded time t*
- Calculate position of blade at t*
- Calculate radiation vector r in blade fixed frame
- Calculate velocity and Mach vector derivative in medium fixed frame and transform to blade fixed frame.
- Find unit normals and tangents to each node on blade, and loading vector depending on choice of source model.
- Calculate derivative of loading vector in ground fixed frame and transform back to blade fixed frame
- Repeat above for each source, evaluate integrals, and add pressure history for each blade

Spectral analysis is then carried out on the combined pressure history of the propeller, and sound pressure levels are calculated.

The flyover noise of the propeller is calculated by applying the above theory at many points during a flyo-

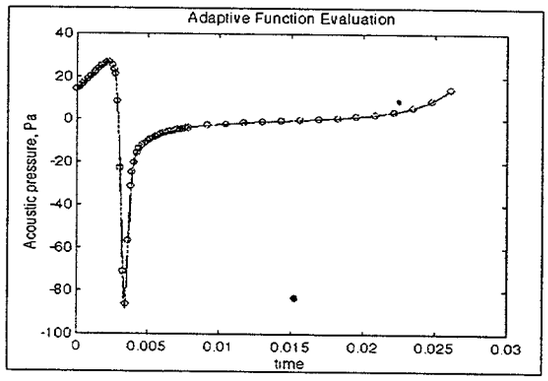

Figure 3 Adaptive function evaluation

gation through the atmosphere and ground effects. The first step is to calculate the Doppler shifted frequencies. Next the attenuation of the sound due to the path length travelled is calculated from the acoustic energy passing through a conical ray tube projected from the source to the observer. The change in characteristic impedance (rc) between source and observer is also taken into account. Following this, the sound attenuation coefficient a, due to atmospheric absorption is calculated using the ANSI method[20]. a is a function of frequency, with temperature, humidity and viscosity being contributing factors to its magnitude. The attenuation coefficient is relatively small, except at higher frequencies, where low Reynolds numbers indicate the importance of viscous effects in the sound field[21].

The last step in the flyover noise calculation involves the calculation of the effect of ground reflection (a result of incident and reflected waves reaching the observer with different phase) and attenuation (absorption of sound by different surfaces) using the ground effect model of Chien-Soroka[22] coupled with the impedance function of Delany-Bazley[23].

Structural analysis is carried out for centrifugal force stress, tension stress, bending stress due to torque load, bending stress due to thrust load and shear stress. Finally, takeoff distance is calculated using the method of Torenbeek[24].

Two methods used to increase cost function evaluation speed

Two approximation methods were carried out to increase the cost function evaluation speed. The first involves the calculation of acoustic pressures for a single blade. As seen above, the sound pressures are calculated for a blade as it completes one rotation. The conventional method used is to divide one rotation into several evenly spaced angles, the solution's accuracy naturally increasing with an increase in the number of points chosen. However,

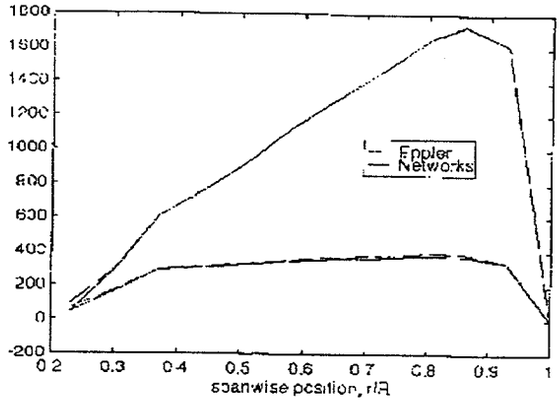

Figure 4 Use of neural networks to replace 2D aerodynamic analysis: Thrust and torque loading

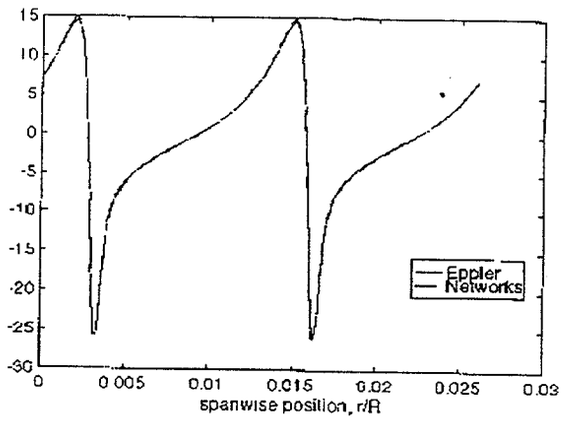

Figure 5 Use of neural networks to replace 2D aerodynamic analysis: Noise

pressure wave form where the change in gradient is high. The procedure is then to first calculate the pressure wave form using a coarse mesh, identify areas where a finer resolution is required, and then recalculate pressures using a fine mesh in these areas. The result is seen in Figure 3. The associated speed increase for this calculation is in the order of 300 percent over a mesh which uses the fine resolution for the entire pressure time-history. In addition, there is absolutely no loss in accuracy.

The next approximation makes use of neural networks[25] to replace the calculation of 2D aerodynamic data, a process which is repeated for ever performance calculation carried out. Neural networks are adaptive mapping systems which map input state space to output state space. There are a number of changeable internal parameters which control mapping characteristics, and supervised learning trains these parameters to produce a desired response for a given system. They are capable of high dimensional, non-linear system estimation, and thus can function as multidimensional, interpolative look-up tables.

Their use in SPONOP involves training networks for several different section types (AraD, Eppler etc.), and have these networks produce lift and drag coefficients when presented with section thickness, angle of attack and Reynolds number. The networks were trained using data obtained from the analysis system described above, over a range of variables which completely cover all possible section operating conditions encountered by general aviation propellers.

Figure 4 compares blade thrust and torque loads obtained by using both the full 2D aerodynamic model and the neural network representation of lift and drag coefficients. Figure 5 shows a similar comparison for acoustic pressure waveform. It can be seen that there is no loss in accuracy, however, the associated speed increase in calculating section properties is in the order of several hundred percent.

Calculation procedure

The order of calculation in the objective function is as follows:

(i) climb performance calculation

(ii) maximum flyover noise level calculation

(iii) maximum attainable speed calculation

(iv) range, endurance and fuel flow calculations during cruise

(v) static thrust calculations, required for takeoff distance calculations

(vi) takeoff performance calculations, required for takeoff distance calculations

(vii) takeoff distance calculations

(viii) cost function calculation and constraint handling

At each of these points the propeller RPM (fixed pitch case) or the blade pitch angle (constant speed case) is solved for by calculating propeller performance over several velocities and RPM's (blade pitch angles). The intercept between THP and propeller power then provides the equilibrium RPM (blade pitch angle). Table 1 shows the governing variables and their values at each design point.

The procedure is identical for every design point except for the maximum speed calculation. Here both velocity and RPM (blade pitch angle) are unknown, requiring permutation of both variables in calculating the propeller performance map. The intercept of this surface

with the THP surface and/or the aircraft power required surface then produces the required variables.

Design point	**Manifold pressure**	**Aircraft Velocity**	**RPM (constant speed propellers)**
Climb	maximum	Velocity for minimum power	maximum
Maximum speed	maximum	unknown	maximum
Cruise	optimised	optimised	optimised
Static	maximum	0	maximum
takeoff	maximum	1.2*stall speed	maximum

Table 1 Values of primary variables in RPM (blade pitch angle) calculations.

The propeller's structure is also tested at each operating point.

The noise calculation block carries out a fly-over noise certification test as per ICAO Annex 16[26]. The observer is positioned at a certain distance from the take-off point, and the noise of the aircraft is calculated for several points as it flies overhead (see previous section). The noise levels are A-weighted and the maximum level is then compared to the aircraft weight based maximum allowable noise level specified by regulation.

Constraints

Simulated annealing is an unconstrained optimisation method which requires the constraints to be added to the cost function. The BFGS based gradient method includes the constraints in its calculation of new search directions.

There are two means of constraining a problem in ASA. The first is to label certain states as invalid, preventing the optimiser from accepting those generated states, thereby leading the search in another direction. Otherwise, constraints are added to the cost function. Constraints applied to the problem in this way include:

- design is incapable of flight in any operating condition due to lack or excess of power
- design is structurally unsound
- design fails fly-over noise test
- design geometry is unrealistic
- specified cruise manifold pressure and RPM are met

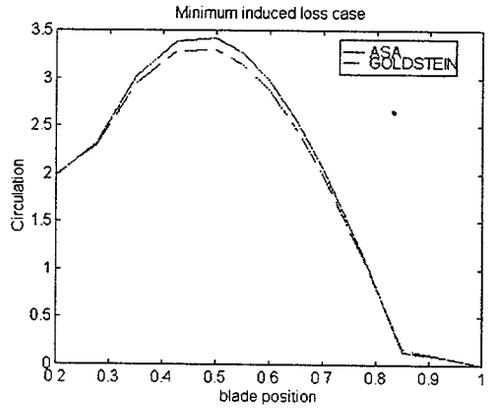

Figure 6 Minimum induced loss circulation for N=3 and λ=0.213

Constraint violation stops are put into position throughout the cost evaluation function, ensuring that the minimal amount of time is spent calculating information for propellers which have violated a constraint. The constraint surface is stepped such that propellers which satisfy all constraints lie in a region well below those which violate one or more constraints. Furthermore, a gradient is introduced into the constraint violation portion of this surface by applying a penalty proportional to the amount which a particular constraint has been violated.

The second stage of the optimiser uses the same constraints as the first and these are applied in the same way. However, additional constraints are required since the generalising functions are no longer used to represent propeller geometry. These constraints require the propeller to have a reasonable geometry, that is, twist and thickness must be decreasing, and maximum chord must be not be located at the tip. These constraints are not added to the cost function, and are handled implicitly by the optimiser. Furthermore, the geometry variables are constrained to remain within five percent of their original values.

Verification

Efficiency

One test case used to prove the optimiser's functionality was the case of minimum induced loss[27]. The propeller is designed for a specified advance ratio and number of blades to minimize the induced loss in the propeller wake. Goldstein[17] calculated the circulation distribution across propellers of varying number of blades and advance ratios, and Figure 6 compares the circulation distribution obtained by the optimiser with that calculated by Goldstein. Agreement is very good showing that the optimiser found the propeller with minimum induced loss.

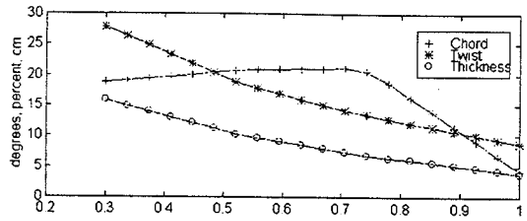

Figure 7 SPONOP propeller geometry

Comparison to an existing design

Table 2 compares the McCauley 1A-200-FA two bladed, fixed pitch propeller installed on a Gippsland Aeronautics GA 200 agricultural aircraft to an optimal fixed pitch design obtained by SPONOP for the same aircraft, engine and number of blades. It can be seen that in all cases the propeller found by SPONOP shows improvement over the off shelf propeller. Furthermore, the SPONOP propeller passes its flyover noise test, the maximum allowable level being 88 dB(A). The SPONOP propeller's geometry is shown in Figure 7.

Variable	McCauley	SPONOP
Rate of climb at velocity for minimum aircraft power required, m/min.	312	332
Maximum speed, kts	86	97
Cruise velocity, kts	81	96
Maximum noise level during flyover, dB(A)	90	87
Takeoff distance, m	543	515
Fuel flow during cruise, L/min.	1.07	0.81

Table 2 Comparison between SPONOP propeller and McCauley test propeller

Each cost function evaluation required 40 seconds using an IBM PR200+ CPU, with approximately 5000 evaluations being required to find the region of the minimum with simulated annealing, and a further 3000 evaluations required by the BFGS gradient descent scheme to find the refined solution.

Conclusion

SPONOP has shown itself capable of designing good propellers in an acceptable time frame on a desktop computer. As such, it is a valuable design tool for small aircraft designers who wish to improve their aircraft performance and reduce flyover noise emission when compared to off-the-shelf propellers. Work is currently underway to use SPONOP to design propellers for the entire range of Gippsland Aeronautics aircraft. These results will be published in a later paper.

Acknowledgments

The authors wish to thank Gippsland Aeronautics Pty. Ltd. for their involvement in this research. The simulated annealing software used in this work was developed by Lester Ingber and other contributors.

References

1. Drack, L. and L. Wood. *Noise Prediction of General Aviation Propeller Driven Aircraft,* in *International aerospace congress*. 1997. Sydney.
2. MathWorks, *MATLAB Reference Guide* 1992, The MathWorks, Inc., Mass.
3. Carlson, S., *Algorithm of the Gods*, in *The Amateur Scientist*. 1997. pp. 105-107.
4. Bounds, D.G., *New Optimization Methods from Physics and Biology*. Nature, 1997. **329**(9): pp. 215-219.
5. Ingber, A.L., *Very Fast Simulated Annealing*. Journal of Mathematics and Computer Modelling, 1989. **12**: pp. 967-973.
6. Ingber, L., *Genetic Algorithms and Very Fast Simulated Reannealing: A comparison*. Journal of Mathematics and Computer Modelling, 1992. **16**(11): pp. 87-100.
7. Ingber, L., *Simulated Annealing: Practice vs Theory*. Journal of Mathematics and Computer Modelling. 1993. **18**(11): pp. 29-57.
8. Winston, W.L., *Operations Research: Applications and Algorithms*. 1994. Belmont. Duxbury Press.
9. Fletcher, R., *Practical Methods of Optimization: Constrained Optimization*. Vol. 2. 1980. John Wiley and Sons.
10. Broyden, C.G., *The Convergence of a Class of Double-rank Minimization Algorithms*. J. Inst. Maths. Applics., 1970. **6**: pp. 76-90.
11. Fletcher, R., *A New Approach to Variable Metric Algorithms*. Computer Journal. 1970. **13**: pp. 317-322.
12. Goldfarb, D., *A Family of Variable Metric Updates Derived by Variational Means*. Mathematics of Computing. 1970. **24**: pp. 23-26.
13. Shanno, D.F., *Conditioning of Quasi-Newton Methods for Function Minimization*. Mathematics of Computing. 1970. **24**: pp. 647-656.
14. Houghton, E.L. and N.B. Carruthers, *Aerodynamics for Engineering Students*. Third ed. 1990. London. Edward Arnold.
15. Eppler, R., *Airfoil Design and Data*. First ed. 1990. Heidelberg. Springer Verlag.

16. Glauert, H., *Airplane Propellers. Aerodynamic Theory.*, ed. W.F. Durand. Vol. IV. 1963. Dover Publications Inc.
17. Goldstein, S., *On the Vortex Theory of Screw Propellers.* Proc. R. Soc. London, ser. A. 1929. **123**: pp. 440-465.
18. Ffowcs Williams, J.E. and D.L. Hawkings, *Sound Generation by Turbulence and Surfaces in Arbitrary Motion.* Proc. Roy. Soc. A. 1968. **264**: pp. 321-342.
19. Lighthill, M.J., *On Sound Generated Aerodynamically. I General Theory.* Proc. Roy. Soc. A. 1951. **211**: pp. 565-587.
20. ANSI, *American National Standard Method for the Calculation of the Absorption of Sound by the Atmosphere.* 1978. American National Standards Institution.
21. Ruijgrok, G.J.J., *Elements of Aviation Acoustics.* First ed. 1993. Delft. Delft University Press.
22. Chien, C.F. and W.W. Soroka, *Sound Propagation Along an Impedance Plane.* Journal of Sound and Vibration. 1975. **43**(1): pp. 9-20.
23. Delany, M.E. and E.N. Bazley, *Acoustical Properties of Fibrous Absorbent Materials.* Applied Acoustics. 1970. **3**(2): pp. 105-116.
24. Torenbeek, E., *Synthesis of Subsonic Airplane Design.* 1990. Massachusetts. Delft. Martinus Nijhoff Publishers
25. Arbib, M.A., *The Handbook of Brain Theory and Neural Networks.* 1 ed. 1995. Massachusetts. The MIT Press.
26. ICAO, *Supplement to Annex 16 - Environmental Protection Volume 1 - Aircraft Noise.* 1990.
27. Larrabee, E.E., *Practical Design of Minimum Induced Loss Propellers.* 1979. SAE TP 790585